5th LECTURE
7th March, 1963.

THE SPARK CHAMBER NEUTRINO EXPERIMENT AT CERN.

by H. Faissner.

1. The problems.

The suggestion to use a spark chamber for the CERN Neutrino Experiment was made by Gilberto Bernardini in fall 1959. The reasons for suggesting such a device for this type of experiment are fairly obvious. The first one is trivial but essential: it seems to be the only way to make a detector which has both a reasonable space resolution and the masses required for quantitative neutrino experiments, where the counting rates are of the order of 1 per ton and day at the very best. The second reason is that the sensitive time is short, say of the order of 1 μsec, and this helps of course in rejecting background from cosmic rays. The third reason is that you can trigger the device by counters, which allows you a certain preselection of events, gives a good time information, and thus helps again in discriminating against background, not only from cosmic rays, but also from the machine.

Therefore, off-hand it seems that the spark chamber counter arrangement may not be so bad. But we have to ask, what information can we get out of such a device for specific questions of physics? Of course, the impressive list of problems which has been given by Bell could, possibly, not be answered completely; but there are a few of them for which a spark chamber seems to be useful. I would like to list them roughly in the order of our preference, which, of course, is to some extent a matter of taste.

1.1 The intermediate boson.

There is first the question of the intermediate boson W.

We do know that the weak four-fermion interaction

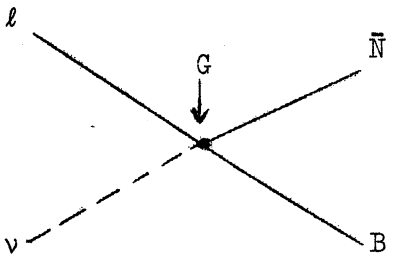

ℓ = μ or e
B = charged baryon
N = neutral baryon
G = weak four-fermion coupling constant (1)

must reveal some structure at high momentum transfers. Splitting it up into two Yukawa-type vertices connected by a boson W

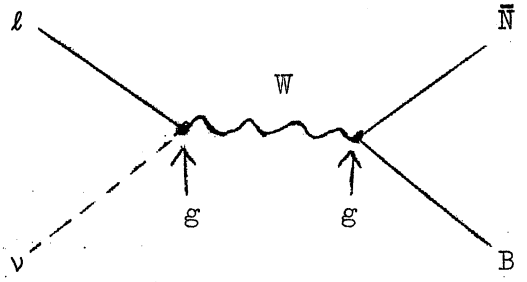

g = "half-weak" Yukawa-type coupling constant (2)

is the simplest way by which you may achieve this structure. Furthermore, if this were true, all interactions in nature (except gravitation) would have the same structure. For aesthetically minded theoreticians this would be appealing. For us it would mean that we could produce the boson as a real particle in a third order process, analogous to electromagnetic pair production,

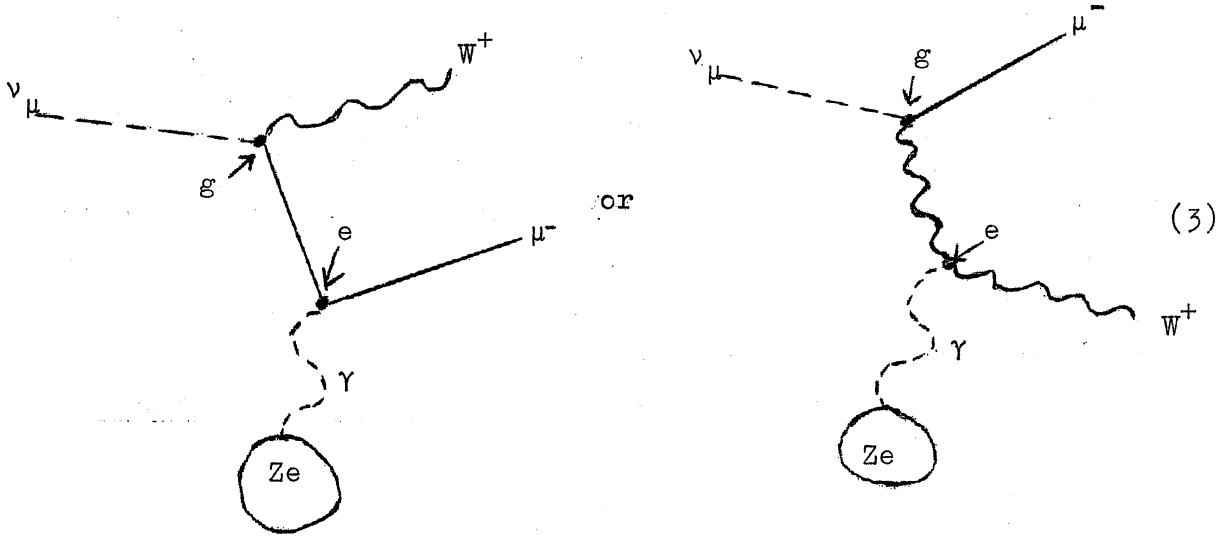

(3)

where momentum is taken up by a nucleus of charge Z. The boson decays rapidly (in $\approx 10^{-17}$ sec) either leptonically

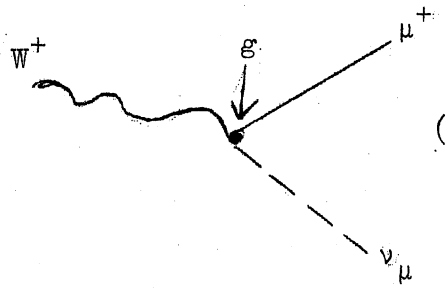

(4) or

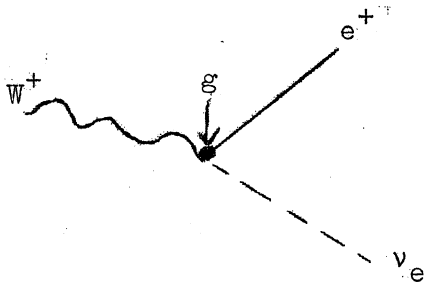

(5)

or mesonically through its link to strongly interacting particles:

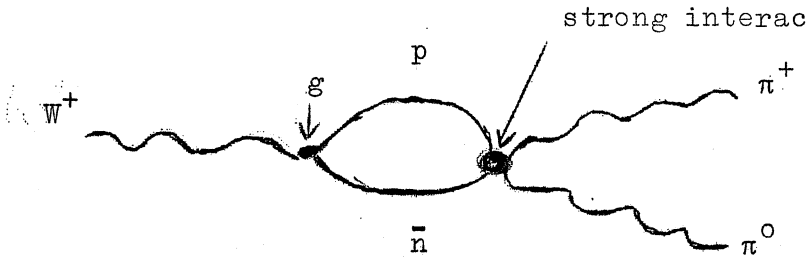

(6)

All this has been discussed by Veltman. The important practical conclusion is that a W^+ production process would appear as a star which contains always a μ^- from the production stage, and in addition either a μ^+ or an e^+ or a $\pi^+ + \pi^o$ from the decay.*

1.2 The one-or-two-neutrino question.

The second problem (historically in fact the first one) is the one-or-two-neutrino question. We may state it as follows: is the neutrino from pion decay capable of producing electrons? The

*Since we can produce the boson at a noticeable rate only if its mass is $\lesssim$ the proton mass, more complicated decay modes, like $W^+ \to \pi^+ + \pi^+ + \pi^-$ or $K^+ + \pi^o$ etc., are not likely to show up in our experiment.

question has found a first answer in Brookhaven, and the answer is NO. It is for this reason that we distinguish the pion-born neutrino by the index μ from its little brother ν_e stemming from beta-decay; and we should call it neutretto (as Puppi did 15 years ago). The existence of two different neutral leptons is a fundamental discovery; and we considered it imperative to confirm it with improved statistics. Furthermore, there is still the remote possibility of a "neutrino-flip", namely that the neutretto, which coupled weakly with the muon forms the pion, is weakly coupled with the electron to form the kaon. Consequently $K_{\mu 2}$ decays would result in ordinary neutrinos ν_e, and we should observe a ratio of electron to muon production corresponding to the respective contribution of kaon - and pion-born neutrinos to the elastic process (5%). As you have heard from Gaillard, the Columbia-Brookhaven group feels that the neutrino-flip is at variance with their data. However, this statement has definitely a lower confidence level than their demonstration of the inequality of ν_μ and ν_e. Finally there will be some electrons produced by ν_e's from K_{e3}- and μ-e-decay. Observing them at the expected rate ($\approx$1%) would be a nice cross check on the two-neutrino-question.

1.3 Form factors due to strong interactions.

In the third place there is the question of the form factors of the elastic reaction:

$$\nu_\mu + n \rightarrow \mu^- + p \,, \qquad (7)$$

$$\bar{\nu}_\mu + p \rightarrow \mu^+ + n \,. \qquad (\bar{7})$$

Determining the form factors is equivalent to measuring the spatial distribution of the leptonic charge of the nucleon. One may call it the Hofstadter-experiment of our days (or rather of the next decade). Lee and Yang have discussed in detail, how one may do it;

(see also the seminar of Løvseth). In particular they pointed out the advantage of measuring the differential cross sections, σ_ν and $\sigma_{\bar{\nu}}$ for neutrettos and antineutrettos separately. This is quite clear: the difference $\sigma_\nu - \sigma_{\bar{\nu}}$ is just the VA interference term and therefore directly proportional to the product of the (total) vector form factor and the axial vector form factor $F_A(q^2)$. If one now believes in the conserved vector current theory, in other words, if one puts the vector form factors $F_V(q^2)$ and $F_M(q^2)$ equal to their electromagnetic values, one can directly extract $F_A(q^2)$ itself. Having the possibility of working at will with either a fairly clean neutretto or anti-neutretto-beam, is one of the great advantages of van der Meer's horn.

So far everything looks straight-forward. Measurement of angle θ and range R of the emitted muons is easy, and even the expected statistics are not so bad (see sec. 5). The difficulty is twofold:

a) One has to discriminate against <u>inelastic reactions</u>:

$$\nu_\mu + n \rightarrow \mu^- + B + \text{anything}, \qquad (8)$$

"anything" being any number of pions, and/or possibly kaons, ρ's, ω's etc. etc.

b) As one is forced to work with complex nuclei (at least for the time being) one has to eliminate <u>nuclear effects</u>. They modify the simple reaction (7) in a very ugly way: the <u>Fermi motion</u> deprives us of the possibility to infer the kinematics from angle and momentum of the emitted muon. <u>Nucleon-nucleon correlations</u> modify even the cross section; (in first approximation one just takes the Pauli-principle into account - but this may be too crude). <u>Secondary interactions</u> of the outgoing nucleon inside the parent nucleus make a measurement of its angle and range rather meaningless.

In brief we fear that our sample of elastic events may

be not very clean. We hope for support from the bubble chamber, where one would see those little stars much more clearly. And we ought to think very seriously how one can measure the elastic process ($\bar{7}$) with free protons.

1.4 Lepton conservation.

Lepton conservation at high momentum transfers is another fundamental problem, one may hope to study to some extent. For this one has to demonstrate the absence of the reactions.

$$\nu_\mu + p \rightarrow n + \mu^+ , \tag{9}$$

$$\bar{\nu}_\mu + n \rightarrow p + \mu^- . \tag{$\bar{9}$}$$

Obviously it requires measuring the charge of the produced muon, and, for a clean experiment, working with a pure neutretto- (or anti-neutretto-) beam. The second condition is not quite met by the horn. There is still a contamination of about 4 % of the "wrong" neutrettos in the beam. But we know this contamination, and may make a more modest check on lepton conservation on a statistical basis: we simply test if the observed rate of μ^+ - production as a function of neutrino energy is compatible with what one expects from the admixture of antineutrettos. Depending on statistics this answer will be good to the order of one per cent. (More subtle violations of lepton conservation, as they have recently been discussed, will escape our observation).

1.5 Inelastic reactions.

The study of the inelastic reactions, in particular of

$$\nu_\mu + n \rightarrow \mu^- + \begin{cases} n + \pi^+ \\ p + \pi^o \end{cases} \tag{10}$$

was mentioned as a pre-requisite for analysing the elastic reactions and the boson production. Moreover, it has some interest of its

own; for instance a careful comparison with pion production in inelastic electron scattering might give another test on the conserved vector current theory. Unfortunately, up to now the theoreticians did not fulfil our hope for precise calculations, but let's hope that they will do so in the future.

1.6 Elastic neutretto - proton scattering.

A sixth and last problem I should like to add for the sake of completeness, namely the question if there is an anomalous neutretto nucleon interaction, which would manifest itself in a true elastic scattering (without charge exchange) :

$$\nu_\mu + p \rightarrow \nu_\mu + p \qquad (11)$$

This looks like a neutral current, but I would like to emphasize that the interaction I am thinking of is not necessarily weak; it could be transmitted by a (boson-) field X

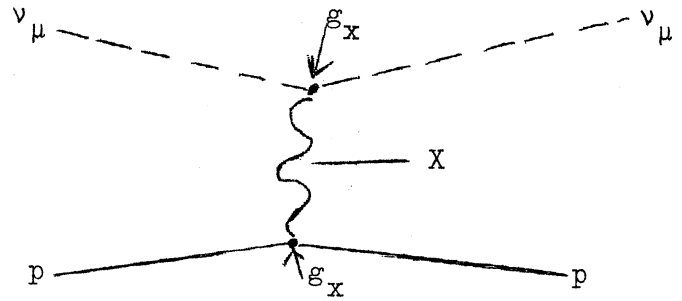

(12)

with a Yukawa coupling constant g_x much larger than the "half-weak" one g associated with the intermediate weak boson W. The new interaction may well be "half-strong"!

All this is highly speculative, but it is of extreme interest in connection with the puzzling question: "Why does the muon weigh?" In fact if one believes the dogma that mass is due to interaction, one has to postulate some interaction for the muon which is not shared by the electron; and it is not

unreasonable to expect the neutretto to show this "muonic type" of interaction too.* In this case the neutretto scattering (11) would be equivalent to the anomalous muon-proton scattering, which is currently under investigation.

Experimentally the process is hard to identify. One has only the proton recoil as a signature. Assuming isotropy in the centre-of-mass, (i.e. infinite X-mass and no form factors for the proton), the average recoil energy is $\approx$ 300 MeV at 1 GeV ν-energy, which corresponds to a range of about 80 g/cm^2 in Cu. A more realistic model* would give even less, typically around 100 MeV $\tilde{=}$ 10g/cm^2, and this would require very thin-walled spark chambers. A terrible background is to be expected from neutron-induced proton recoils. Nevertheless, an upper limit for neutretto-proton scattering around 10^{-36} (perhaps 10^{-37}) cm^2 might be within our present possibilities. I hope we hear more about it in one of the later seminars.

Table I summarizes the problems and their experimental implications. In brief, the study of the elastic reaction, inclusive the related question of lepton conservation, requires the analysis of tracks, (defined as one approximately straight line of sparks corresponding to a range R of $\gtrsim$ 100 g/cm^2). The two-neutrino question and also the boson, imply on top of that the identification and measurement of showers. In three of the problems: boson, inelastic processes, and to some extent elastic

---

* After the seminar was given, the speaker discovered that Okun and his co-workers have already worked out a complete theory of this half-strong interaction:

I. Yu. Kobzarev and L. B. Okun, J.E.T.P. 41 (1962) 1205
[= Soviet Phys. JETP 14 (1962) 859]
V. V. Mandelzweig, J.E.T.P. 42 (1962) 1278
[= Soviet Phys. JETP 15 (1962) 886]

There was even a neutrino experiment performed at Dubna on this question, yielding an upper limit on the cross section of (11) of $\approx 10^{-32}$cm^2:

I. M. Vasilewsky et al., Physics Lett. 1 (1962) 345.

TABLE I

The problems and their experimental implications.

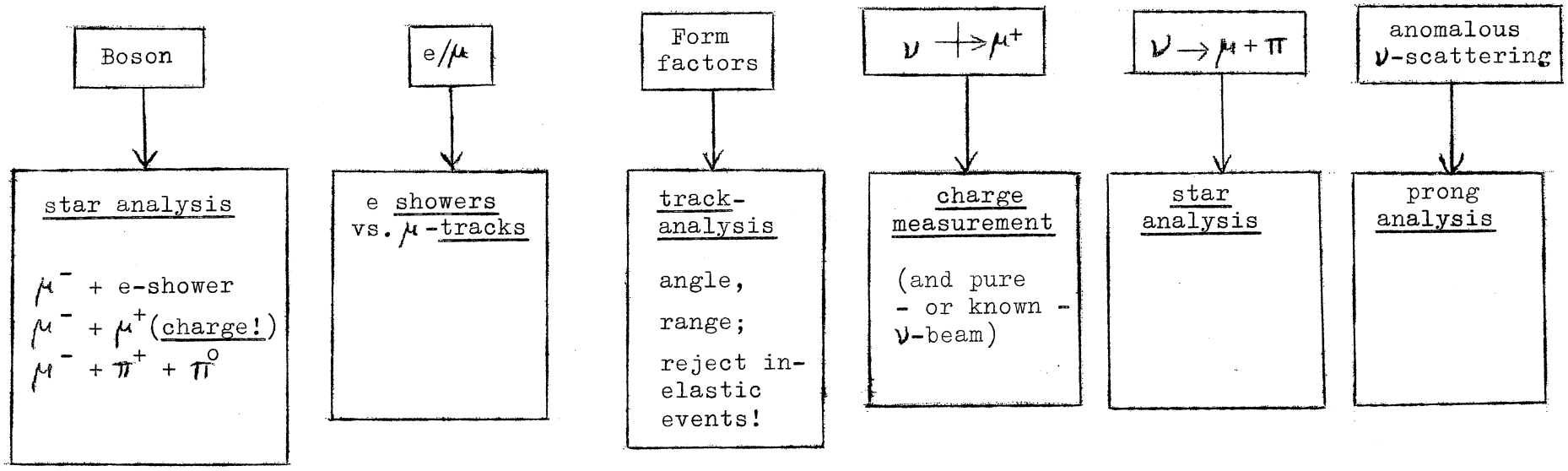

ones, one has to analyse stars. Study of neutretto-proton scattering instead requires analysis of prongs ($R < 100\ g/cm^2$). Charge measurement, i.e. a magnetic field, is imperative for the lepton-conservation, and for the boson, if you put your money on the muonic decay channel (4).

When you look at this list of problems and their implications, you have to make your mind up, on which problem you want to concentrate, and you can either design a set-up which is good for one problem, or two, and not good for the others. Alternatively you could try to make a flexible system, in other words a compromise, and you hope to get out a little bit for everything. Up to now we have chosen a compromise, and I want to describe today on which grounds this compromise was arrived at, and what its possible advantages and its obvious short-comings are. I shall not go into any technical details, because most of the experts are here in this room. Also I shall not try always to give proper credit, because many people were involved, and the turnover-rate was high (see Appendix I).

2. The spark chamber modules.

2.1 Conflicting requirements.

The practical implications of the considerations outlined above may be stated in terms of two experimental parameters: the material and thickness of the chamber plates, and the spacing of the triggering counters. The first one determines the accuracy of the analysis, the second one the efficiency of detection. Clearly, the problems mentioned require widely different arrangements: analysis of prongs and stars calls for thin and light plates and for a close counter spacing. Analysis of showers, (either from directly produced electrons or from gammas from π^o's), although still requiring close counter spacing, is better done with thin and heavy plates; (where "heavy" really means

high Z!) The reason is that we want to have electron showers of high multiplicity. Now, any shower theory gives for the total number of electrons N_e (above a certain cut-off energy of some MeV), produced from a single electron (or γ) of energy E_o, the following order-of-magnitude relation:

$$N_e (E_o) \approx E_o/\varepsilon \tag{13}$$

where ε is the critical energy. The multiplicity $\bar{n}$, averaged over the whole range of the shower R_o is then

$$\bar{n} = \frac{Ne}{R_o} = \frac{E_o}{\varepsilon R_o} \tag{14}$$

Remembering that the range, as measured in radiation lengths, does not depend on the material, we may derive from (14) the scaling law for the multiplicities in two different materials 1 and 2:

$$\frac{\bar{n}_1}{\bar{n}_2} = \frac{\varepsilon_2}{\varepsilon_1} , \tag{15}$$

i.e. the multiplicity as well as the total number of produced electrons N_e is inversely proportional to the critical energy. This argument is independent of the way one samples the shower: of course one gets more information if one makes the plates thinner and thinner, but in case $\varepsilon >> E_o$ the electron just does not multiply; it stays a track, and neither is there a distinction from a muon nor a meaningful correlation between the total number of observed sparks and the initial energy E_o.

Finally, turning to the problem of analysing tracks, we encounter again different requirements. We remember that typical ranges of muons from the elastic reaction amount to many hundred grams/cm^2. Furthermore, we distinguish muons from pions by the absence of nuclear interactions, for instance large angle

scatters or stars. Again this requires path lengths of several 100 g/cm^2. Therefore, for track analysis the plates have to be thick; the counter spacing can be correspondingly large.

2.2 The solution: modular spark chambers.

Our practical solution is quite simple: we built 3-plate modular spark chamber units of two types

A with 5 mm aluminium plates,

B with 5 mm brass plates,

which seemed to us a reasonable approximation to what we called above thin and light, and thin and heavy, respectively.*) The thickness of 5 mm was the minimum we found compatible with our requirements of flatness for proper spark chamber operation: since the gap width is 1 cm, the deviation from flatness must not exceed some 0.1 mm. A thick plate chamber can be realized by interposing lead or iron walls with either A- or B- modules.

The lateral dimensions of the chambers are a compromise between our desire for large size, and the limitations of this earth. In the vertical dimension we were limited by anticoincidence counters and shielding to 160 cm. The horizontal dimension was limited to 100 cm, because European factories would not easily roll aluminium or brass sheets larger than that. As this width was considered too small, we decided to use two rows of chambers and to place them side by side. Table II gives some properties of the spark chamber modules, and also of the triggering plastic counters.

Fig. 1 shows the construction of a 3-plate module (due to Frank Krienen): the two grounded plates are glued together with some metal distance pieces to form a mechanically stable box. The central plate, on which the positive high voltage pulse is applied, is supported by six plexiglass insulators, which are introduced through gaps between the distance pieces. There are sometimes discharges

*) From the ratio of the critical energies (54 and 26 MeV respectively) one expects a factor of 2 in electron-multiplicity, when going from aluminium to brass.

TABLE II

Some properties of the modules (1.6 x 1.0 m^2)

Type	A	B	C
Material	Al	brass	plastic scintillator
Thickness in cm	3 x 0.5	3 x 0.5	2
" in g/cm^2	3.8	13	2
" in MeV	6.3	19	4
Weight (kg)	60	200	32
No. of units per ton	16.5	5	31.5
" " " " radiation length	6.5	1	20
" " " " interaction length	20	8	26

across these insulators. Small teflon sheets have been inserted in order to depress them (see detail). The modules, together with the triggering counters and, if wanted, with additional absorbers, are assembled on small chariots, which can take up to 9 three-plate spark chambers each.

2.3 Our experience with the modules.

During the past year several arrangements of modular spark chamber units have been tested in various beams at the CERN proton synchrotron. We wanted to get some feeling how elementary particles look like in our chambers and so we took many kilo-pictures of practically all reasonably stable particles: γ; $e^{\pm}$; $\mu^{\pm}$; $\pi^{\pm}$; π^{o}; K^{-}, K^{o}; p, $\bar{p}$, n and d. Admittedly all charged strongly interacting particles look quite similar; they make stars, or suffer large angle scattering; except of course the antiprotons, which make spectacular annihilations; but otherwise there are rarely more specific reactions, like a π^{-} transforming itself into a π^{o}, or a K^{-} producing a clearly discernible Λ. Muons, on the other hand, have a quite distinct appearance: metres of tracks, often curved by multiple scattering, sometimes accompanied by small knock-on electron showers; but never ending in a star, and never showing large angle single scattering. Fig. 2 shows a typical muon track.

Particular emphasis was placed on the identification and measurement of electrons. After considerable work, spent on improving the multiple particle detection efficiency, we arrived at pictures like fig. 3. It shows an electron of 2 GeV initial energy entering the chamber-counter assembly from the left.*) One even sees details of the shower development: the primary electron suffered a violent bremsstrahlung loss immediately in front of the fifth gap, and one sees the radiated quantum converting two chambers later. The generated pair, because of its small opening angle, forms just one track at the start; later on electron and positron

*) It is already the final "production" assembly: 2 Al-chambers followed by a brass chamber and so on with some plastic counters in between.

get separated by multiple scattering, one of them even going far outside the shower core. The fact that one can follow one and the same electron through several subsequent gaps shows that they have still reasonably high energies during the first few radiation lengths, (in agreement with equ. (13)!); it demonstrates further the high detection efficiency eventually achieved. Only towards the tail of the shower there is a preponderance of uncorrelated, scattered around sparks, due to low energy electrons. Finally, at very large depths, we are left with a few insulated sparks, mainly caused by Compton-electrons from photons near the "hole" in the absorption cross section.

The primary energy E_o can be determined from the total number of sparks N. If one spark corresponded to one electron, and vice versa, N would be essentially proportional to the total number of electrons N_e. Alternatively, if every spark was part of a track, we would measure the total tracklength L_t. Our case is in between the two extremes, but is somewhat closer to L_t. Fortunately, both quantities, N_e as well as L_t, are supposedly proportional to E_o. Therefore our measured number of sparks should be proportional to E_o also.

Unfortunately, there are a number of systematic effects which disturb this nice linear relation: as we have seen, an energetic pair gives only one spark per gap; one spark may be hidden behind another one; faint sparks are being lost with small camera apertures; the efficiency for sparking does still depend on number and distance of other sparks etc. etc. This altogether makes electron-spectroscopy with spark chambers a rather tricky affair. Since Beat Hahn will give a full seminar about this topic, I stop here. Let me just give two approximate numbers: the relative accuracy of the energy determination from the total spark number is $\approx$ 15% for one electron of $\approx$ 1 GeV. If we ask for the lowest energy at which we are able to distinguish an electron from anything else with good confidence (say $>$ 80%) I would guess

300 MeV. (400 MeV is already certain). To finish this excursion about the properties of the spark chamber modules let me show another picture exhibiting an elastic charge exchange of a 4 GeV/c π^- in CH_2 (fig. 4).

3. Geometry of the neutrino set-up.

The arrangement chosen for the next phase of the neutrino experiment comprises several sections, each of which is meant to take over one of the tasks mentioned above (see fig. 5): the first part of the set-up is the "light production region", consisting of aluminium and brass chambers with a counter spacing sufficiently close to have a detection efficiency of $\approx 2/3$ for 600 MeV electrons. This region is therefore good for shower-, star-, and (to some extent) prong-analysis. It is followed by the "heavy production region" which is made up essentially of brass chambers, with a few widely spaced counters. This part of the set-up is simultaneously an analyser for tracks leaving the first part, but more important: it constitutes a high density target concentrated in front of the magnet. This consists of a pair of Helmholtz coils with a few sampling aluminium chambers inserted. Its only function is to establish the sign of the particles emerging from the production region, in particular to reveal the $\mu^+\mu^-$ - pairs typical for a boson-production. The set-up is closed by a thick-walled range-chamber, realized by some spark-chamber modules with lead or iron walls in between. It serves mainly for distinguishing muons from pions. Some technical details about these different sections are given in the following.

3.1 The light production region.

This consists of a mixture of aluminium (A)- and brass (B)-chambers in the ratio 2:1 (in number). Interposed with them there is a fairly large number of triggering plastic counters (C). Their size is also 160 x 100 cm^2, and each of them is composed of four sheets of 80 x 50 cm^2. The sheets are individually viewed by a single 53 AVP 2" photo multiplier. Because we have to photograph

from the side, the phototubes are mounted on top and bottom of the assembly.

On each chariot the units are mounted as follows:

ν →	A	B	C	A	A	B	A	A	C	B	A

(16)

In this way the chambers follow each other always in the sequence BAA. There are four chariots on each side (fig. 6). Each of them carries a detector mass of one ton, giving 8 tons in total.

The thickness of the light production region is 260 g/cm^2, corresponding to an energy loss of 400 MeV for a minimum ionizing particle. Since the distance between adjacent plastic counters is either 28 or 34 g/cm^2 (i.e. 44 or 51 MeV) the detection efficiency for muons from elastic reactions is practically 100 %. As measured in radiation lengths the distances are 1.6 and 2.3 Xo. Even if we require coincidences between adjacent counters, this ensure a detection efficiency of about 2/3 for a 600 MeV electron. As already discussed, the discrimination between electron and heavier particles is good from 300 MeV up, and the energy measurement is fairly accurate. Since a typical recoil proton momentum in the elastic reaction is ≈ 500 MeV/c, (corresponding to 130 MeV kinetic energy), it could transvers 1 Aℓ + 1 brass-chamber in the normal direction. Allowing for the inclination one would still expect to see about 3 or 4 sparks on the average. Also some of the more energetical recoil protons from the hypothetical anomalous scattering process (11) are expected to show up. The analysis of stars is fairly detailed.

3.2 The heavy production region.

All the chambers are brass, and there is only one plastic counter per chariot. The other counter frame was filled with 2.5 cm thick iron plates, partly because of increased mechanical stability, but mainly because we did not like to waste space which could be filled with matter. The sequence on a chariot is:

ν →	B	Fe	B	B	B	B	B	C	B

(17)

There are 6 chariots of this type. (Actually some of them differ somewhat from (17), in as much as the two B-three-plate chambers to the inside of C or Fe have been replaced by one five-plate chamber.) The two closing chariots instead carry 4 three-plate chambers followed by a liquid scintillation counter L_1. (This has no deeper reason; we simply ran out of plastic counters.)

The total weight in this region is 12 tons (including the iron). The thickness is 385 g/cm^2 corresponding to 570 MeV energy loss. The detection efficiency for muons is still close to unity. For electrons it is negligible. Nevertheless, the analysis of showers accompanying penetrating particles is still feasible. To some extent this is also true for accompanying stars.

3.3 The magnet.

This is a Helmholtz-type pair of coils supplying 4 kGauss (= 0.4 Wb/m^2), at the maximum current of 2500 A, over a region of length 2ℓ = 130 cm, and a cross section of 120 x 110 cm^2. The particle trajectory is measured in Aℓ - chambers at 5 points (or four, if the particle misses the last chamber). This is illustrated in fig. 7, which is taken from an internal report (NP/NEU 4) by Jean-Marc Gaillard. One easily convinces oneself that in the case of small deflection angles θ, the sagitta of the circular part of the path s is given by

$$s = \ell' \frac{\theta}{4} \qquad (18)$$

where $2\ell' = 0.76 \times 2\ell$ is the effective length of the field region. s is 1.9 cm for a 1 GeV/c particle. The relevant sagittae, however, are S or S' ($\approx$ S"), and since they attain respectively values of about 9 and 4 cm, the estimated total error of respectively 10 and 8 (6) mm, permits a momentum measurement of 10,20 (15) % accuracy at 1 GeV/c. The maximum detectable momentum is about 10 GeV/c, and up to this value the charge measurement can be done with $\geq$ 97.5 % confidence; (97.5 % at 10 GeV/c if S is measured).

A magnetic shielding wall of 15 cm Fe prevents the stray field from disturbing our photomultipliers in the production region (see fig. 5). Fig. 8 is a photograph of the magnet set-up.

3.4 The range-chamber.

This consists mainly of lead and iron walls, thinner ones at the beginning, very thick ones at the end. Fig. 9 shows them in the stage of being mounted. Between two subsequent walls one 3-plate chamber is inserted. In principle one could take either Aℓ or brass modules. But the light Aℓ-chambers are easier to mount. The sequence is as follows:

$\nu \rightarrow$ 4 x 5 cm Pb, 5 x 10 cm Pb, 2 x 15 cm Pb, 20 cm Pb; 2 x 20 cm Fe. (19)

Originally the only purpose of this chamber of 1680 g/cm^2 ($\tilde{=}$ 1984 MeV minimum energy loss) thickness was to have pions (and other "stronglies") interacting, and muons either penetrating or stopping. However, since the seminar was given, an increasing number of group members felt that it was a pity to waste the total 53 tons for just this purpose. Therefore, plastic counters were inserted into the two 15 cm walls, and a liquid counter L_2 was installed behind the chamber (see fig. 5). In this way muons (and muon pairs!) produced in the range chamber are detected with about 1/3 efficiency.

3.5 Photography.

The set-up as it stands now (mid-June 1963) comprises 244 spark-chamber gaps of 1.0 x 1.6 m^2 in the production region, 52 in the range chamber, and 14 in the magnet; in total 310*). Its total length from the beginning of the production region to the end of the range-chamber is 10.5 m. To photograph this monstrosity is not an easy matter.

*) For comparison: the Brookhaven set-up had 90 gaps of 1.2 x 1.2 m^2.

I have neither the time nor the competence to discuss all the many arguments which have been put forward (and withdrawn). But looking back, it seems to me that eventually the following postulates have prevailed:

a) the photography should be straightforward, in the sense that the image on film does not differ too much from what one sees in object space by eye.

b) the system should be flexible enough to accommodate any arrangement of modules.

c) the accuracy should be close to the natural one, which is given by the spark width (≈ 1 mm).

d) scanning and reconstruction should be easy.

I do not claim that the actual discussion proceeded in such logical terms, nor do I claim that the adopted solution follows logically from the postulates. However, postulate a), together with the need for stereoscopy, does make two pairs of cameras, for the two rows of production chambers, a very natural solution (see fig. 5). The TOP (BOTTOM) cameras are at the height of the upper (lower) edge of the spark chambers. 35 mm film is used. A special consequence of a), namely the postulate of equal demagnification (1:57) for all parts of the set-up, made the virtual camera positions for the range chamber fall into inaccessible places. Large mirrors had to be introduced (fig. 5). The stereoscopy in this region (and also for the hodoscopic-chambers in the magnet) is done by mirrors, which bring TOP and BOTTOM view on the same (70 mm-) film.

The trivial and difficult problem, to look into the chambers parallel to the plates, was solved by mounting a pair of thin flat mirrors in front of each spark chamber. The principle of operation is illustrated in fig. 10, and one convinces oneself easily that the deflection angle between initial and final ray depends only on the relative angle between the mirrors α, not on their orientation with respect to the spark chamber plates.

That the system, when properly adjusted, works perfectly, is demonstrated by fig. 3: on the left hand side of this picture the mirrors were mounted; on the right hand side they were taken away. The system (devised and realized by Muratori) has occasionally been accused of being too complicated and delicate - unjustifiedly, it appears to the speaker. If one takes the postulate of flexibility seriously, in particular if one wants also the possibility of large-angle photography, plexiglass prisms cannot be used. The only other possibility would have been to make a fan-shaped arrangement of spark chamber modules, but this would have made a very ugly detector structure which would have violated requirement d). (The proposal to tilt not the single modules but only the carriages, would have had the same inconvenience, plus the necessity of working with multiple reflections from the spark chamber plates - i.e. replacing glass mirrors by scratchy metal surfaces!)

The accuracy requirement c) implies a careful selection of mirrors. If this is done, the vertical co-ordinate in object space may be determined with an absolute error of ± 2 mm in the production region, ± 1 mm in the magnet, and ± 3 mm in the range-chamber. The accuracy in the depth co-ordinate z is a factor of 4 worse. As it was found in the electron pictures, two weak sparks can be resolved if their projected distance Δy is $\gtrsim$ 3 mm.

Main reference marks are horizontal and vertical nylon wires. They are illuminated after each exposure, together with the mirror edges, by some suitably arranged lamps.

3.6 Anti-coincidence counters.

These are mounted on top of the production region, (20 m^2), and in front of it (10 m^2). The counters are plexiglass boxes, (dimensions: 200 x 85 x 18 cm^3 for most of the FRONT counters; 250 x 100 x 30 cm^3 for the TOP), filled with decalin- or Shell Sol A- scintillator, and loosely wrapped in Al foil.

They are viewed by two 5" 54 AVP photomultipliers mounted on one of the small sides.

The anti-counters were indispensable, when we planned to run with a longish burst from an internal target. Even now they might be useful - not so much against cosmic rays, as the gated rates are low - but for rejecting stray muons from the machine.

4. Operation of the set-up.

Whereas the preceding section had to do with the space-like aspects of the set-up, the present one will deal with its behaviour in time. This will amount to a brief description of the electronics.

4.1 The logical electronics.

This selects combinations of counter pulses which might signalize a neutrino event. It is conventional (in fact to a large extent composed of standard Nuclear Physics Division units), moderately fast, (resolving time of the coincidence units 16 nsec), and of course fully transistorized.

A simplified block diagram is sketched in fig. 11: the signals of the 8 sheets (80 x 50 cm^2) of a complete plastic counter (160 x 200 cm^2) are separately brought into the electronical control region (behind the back shielding wall of fig. 5) where they are combined by an active adder and amplified in two fast amplifiers. The basic YES-signal from the production region is a coincidence between two adjacent plastic counters (P_k, P_{k+1}). All these signals, together with the single counts from the liquid scintillation counter, are collected in an OR-gate and fed through an anti-coincidence unit, with the combined TOP and FRONT-signals at the NO-input. After that they are combined with a completely analogous line from the range-chamber, by another or-gate, and reach finally the CENTRAL DISCRIMINATOR. This unit is gated with a 2.5 μsec pulse synchronized with the radiation from the

neutrino horn. The output of this gated discriminator is split into a number of outputs which give trigger signals to the "actuating electronics" (see below).

Not shown in fig. 11 are some fine points, like a paralysis unit avoiding spark chamber overloading, another paralysis system preventing scalers from counting sparks, and a test system, consisting of a cosmic ray "master trigger" $M = (P_1, P_2, P_{11})$, which, fed back to the normal $(P_k\ P_{k+1})$ - units (in fact triple-coincidence-units), allows the efficiency of each plastic counter P_k $(k = 3...10)$ to be measured by comparing (P_k, M) with M. There is also provision made to trigger (on an independent line) on large single counts from the plastics P_k, in case this should be feasible and desirable, (for instance in order to have higher detection efficiency for short ranged events).

4.2 The actuating electronics.

This initiates the various actions which have to be taken after the occurrence of a suspected neutrino-event:

a) the master spark-gap is fired through a EFB60 trigger followed by a hard tube. The output pulse in turn fires the $\approx$ 20 spark-gaps, mounted close to the chambers, which switch the high voltage onto the chambers. One spark-gap usually supplies 8 three-plate-modules, but every module has its own high-voltage condenser of $\approx$ 4 times the module-capacity. The spark-gaps are of the so-called "two-electrode" type (with an ignition-electrode placed into a central boring in one of them). Frank Krienen devised them utilizing the experience of Kuyper and Plass. No corona is employed; (one never gets it stable!) The gaps are metallically closed off and can be pressurized, (though, at present, they work beautifully with standard air).

The rise time of the high voltage pulse at the chamber plates is mainly determined by the (low!) eigen frequency of the LCR - network. It is about 35 nsec. (Though, without load, the

spark-gaps alone break down in 10 to 20 nsec.) The total delay, between the passage of a particle and the appearance of the high voltage on the chamber, is ≈ 460 nsec. 140 nsec are spent in the high-voltage trigger units (tube-circuits + the two spark-gaps); the rest is cabling and logics.

b) The illumination system for the reference marks is switched on for a few tenths of a second.

c) Hollerith information (frame number, measurement number, number of accelerated and ejected protons, etc.) is put on so-called "digilights" and thereby brought onto the photograph.

d) A coincidence display marks by flashing up of little lamps, which counter coincidences (or single counts in the case of liquid counters) were responsible for the trigger. This gives a very desirable possibility of checking counter behaviour versus spark-chamber tracks.

e) The camera advance is initiated.

4.3 The time-of-flight measurement.

This is an elegant way of utilizing the bunch structure of the radiation. The "event"-signal from the central discriminator starts a time-to-pulse height converter. The STOP-pulse comes from a signal which is rigidly clamped to the bunch phase; (actually it is just the phase of the RF acceleration voltage). Thus the time-of-flight of every registered particle is measured (modulo the bunch-period of 105 nsec and up to an uninteresting constant delay). Also this number is photographed for each event. This gives us the possibility of deciding if a certain class of events is mainly due to neutrinos, or if there is a contamination of slower particles: neutrino-induced events must show a time-of-flight distribution whose width is mainly given by the width of the PS bunches and whose position must coincide with the one obtained from muons penetrating the shielding (at enhanced PS energy, say). Any neutron

contamination would manifest itself by a tail on the "late" side of the distribution. The usefulness of the method may be judged from fig. 12, which demonstrates a separation of pions and protons, achieved in a PS beam of 2 GeV/c with this method and a flight path close to that of the real neutrino experiment (≈ 60 m).

4.4 An automatic test system.

This is also foreseen for a later stage. It would register, and automatically read out, the natural single counting rates (cosmics + noise above a fixed level) of all photo-tubes employed, and also, if wanted, of certain signal-combinations.

5. Expected rates.

Let me finish by briefly stating the rates one expects to find with our set-up:

5.1 The elastic reaction (7).

I shall give all neutrino induced rates for a reasonably optimistic PS-intensity of 4×10^{11} circulating p per burst*). Lee and Yang's cross section together with van der Meer's spectrum give then at the position of the spark chamber a rate of

4.25 elastic events/d and ton

For the 20 tons of the production region this gives

85 el. events/ day or 3.5 el. events/hour.

But only ≈ 80% i.e. 68/d or 2.8/h will fall inside the fiducial volume and only ≈ 1/3 of them will stop.

The range-chamber with its approximately 20 effective tons will contribute the same amount of elastic triggers. It remains to be seen, how many of them are really useful for the analysis.

*) At the time of writing the PS runs steadily at 6.5×10^{11} circ. p per burst.

Inelastic events, according to Brookhaven, are about as frequent as elastic ones. This gives, even without boson production, a neutrino trigger rate of about 15/hour.

5.2 Boson production.

Here I shall be brief, because Roberto Salmeron has more to say about it. From what I understand from him, I get a production rate for a 600 MeV boson which is somewhat higher than the elastic rate. Instead, the rate for a 1 GeV boson is by some factor (2-3 or so) lower than the elastic rate.

What I want to give is the branching ratio for W-decay into the leptonic channels and $\pi^+ + \pi^o$. (Other channels are neglected.) The conserved vector current theory gives (according to formulae of Bernstein and Feinberg):

Boson mass	$W^+ \rightarrow \mu^+$	$W^+ \rightarrow e^+$	$W^+ \rightarrow 2\pi$
600 MeV	1/3	1/3	1/3
1 GeV	0.40	0.40	0.20

The muonic channel is the interesting one for us. For the $\approx$ 10 tons of spark chamber in front of our magnet Ghani has calculated the geometrical efficiency that the decay muon goes through the magnet. He finds typically 10 - 15%.

Thus we may hope for about 6 analysable bosons of 600 MeV per day; a rate which may drop to about 1 per day in case the boson has a mass of 1 GeV.*)

---

*) The latest values of Salmerons give (for 10 effective tons and 4×10^{11} circ. p / burst M_W = 600 MeV: Produced = 120; μ-decay = 40; though magnet = 6 per day. - For M_W = 1 GeV, the figures are respectively: 32, 13 and 1.3.

5.3 Cosmic ray background.

An upper limit for the muon rate in the production region is readily obtained, if one assumes that all muons transversing the spark chamber set-up are actually detected: the surface of 6 x 10 cm^2 and a flux of 0.8 x 10^{-2} sec^{-1} cm^{-2} give a rate of 500 sec^{-1}. The top shielding of 250 g/cm^2 Fe + 550 g/cm^2 concrete reduces this to $\approx$ 200 sec^{-1}. With an anti-efficiency of $\approx$ 50% this gives $\approx$ 100 sec^{-1} as ungated trigger rate. With a 2.5 μsec gate applied all 3 sec we find 0.8 x 10^{-4} cosmic muon triggers per burst or 1.5 per day (!). We gain another factor of 5 from the bunch structure. If 5% of the muons would stop in the chamber and simulate a neutrino event (Brookhaven figure 2%), we had only 1 cosmic muon background event in 80 days.

The enormous duty factor which works in our favour does also depress the rate of strongly interacting cosmic rays to an absolutely negligible level. Starting with a flux of $\approx 10^{-4} cm^{-2} sec^{-1}$, and repeating (slightly modified) the same trivial computation one arrives at a rate of 5 x 10^{-4} interacting cosmic stronglies per day.

5.4 Background from the PS, as we know, is hard to estimate. Although the shielding is much better than it ever was in the past, we may have surprises. Nevertheless, with our improved diagnostic apparatus, we may also find a therapy.

APPENDIX I

Scientists in the neutrino-counter-spark chamber group:

L. Cucancic (Nov. 60 - May 62),
H. Faissner (from May 60),
F. Ferrero (Nov. 60 - July 62; Visitor Dec. 62 and from April 63 on)
C. Franzinetti (from Nov. 62)
S. Fukui (from Sept. 62)
J. M. Gaillard (from Nov. 62)
H. J. Gerber (from June 62)
A. Ghani (from Summer 61)
B. Hahn (from October 62)
E. Heer (Sept. 61 - June 62)
R. Hillier (from October 62)
F. Krienen (from July 61)
G. Muratori (from October 61)
T. B. Novey (Sept. 61 - June 62; visits in 63)
M. Reinharz (from Sept. 60)
R. A. Salmeron (from July 61).

APPENDIX II

Papers and Reports about the subjects discussed:

"The Neutrino Spark-Chamber",
Nucl. Instr. and Meth. 20 (1963) 213;
"Spark-chamber efficiency for electron shower detection" ibid. p.161;
"Performance of large liquid scintillation counters" ibid. p.289.

Reports about the plastic counters, the time-of-flight method, further multiple particle efficiency measurements, the optics, spectroscopy of electrons and gammas (und anderes mehr) are in preparation.

FIGURE CAPTIONS

Fig. 1. Construction of the modular spark chambers.

Fig. 2. Typical muon track.

Fig. 3. A 2 GeV electron multiplying in the chamber set-up.

Fig. 4. A 4 GeV/c π^- transforming itself into a π^o in a CH_2 target.

Fig. 5. Geometry of the neutrino spark chamber-counter arrangement.

Fig. 6. View of the production region.

Fig. 7. Principle of the measurement of magnetic sagitta in the Helmholtz coils. Field region extending to $\pm \ell$ from the centre (0). Measurement of 5 points in space, (or 4, if the particle does not hit the chamber at the exit = right-hand side of sketch).

Fig. 8. The magnet coils seen from the side. Note the pair of spark chambers at the entrance (right-hand side) and at the exit (left-hand side) of the coils, and the two single chambers in the field region (the third one is covered by the pillar in the foreground).

Fig. 9. The range chamber in the stage of construction. One of the 5 cm lead plates may be seen on the right-hand side.

Fig. 10. Principle of the mirror optics.

Fig. 11. Schematic block diagram of the electronics.

Fig. 12. Time-of-flight spectrum of a +2 GeV/c PS beam, (flight path $\approx$ 60m), using the bunch structure of the emitted radiation.

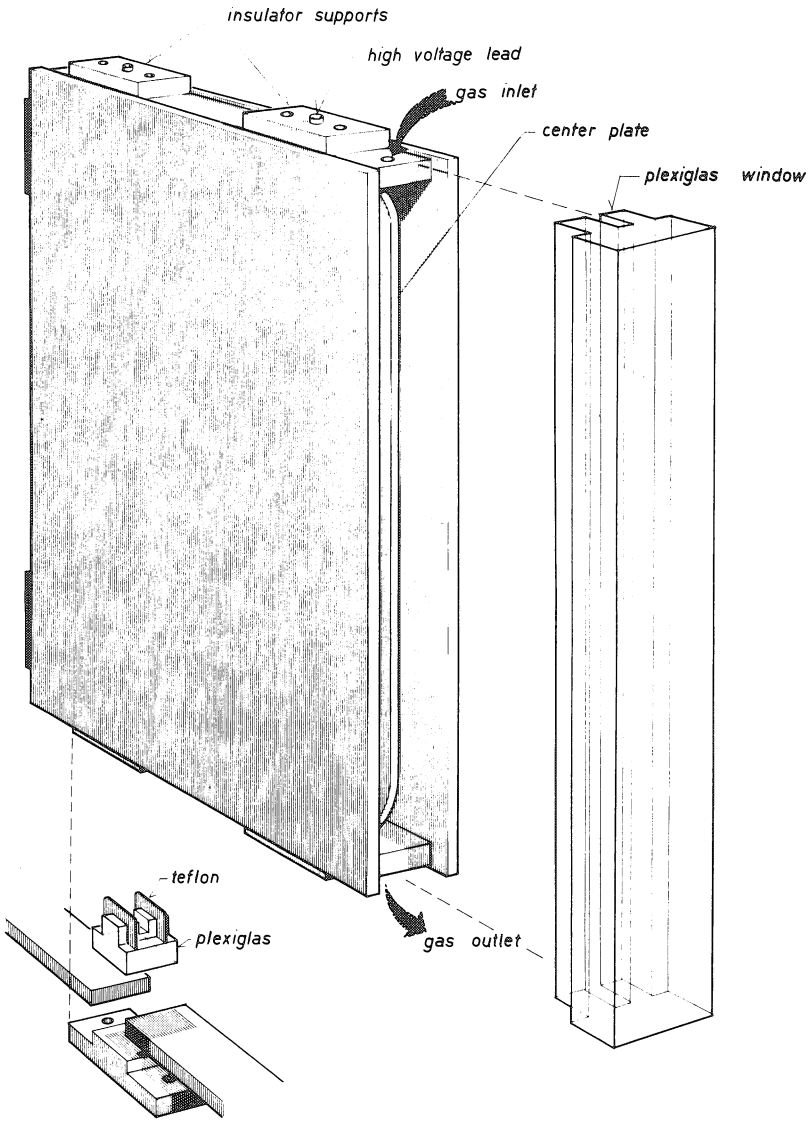
insulator supports
high voltage lead
gas inlet
center plate
plexiglas window
teflon
plexiglas
gas outlet
DETAIL INSULATOR

Fig. 1

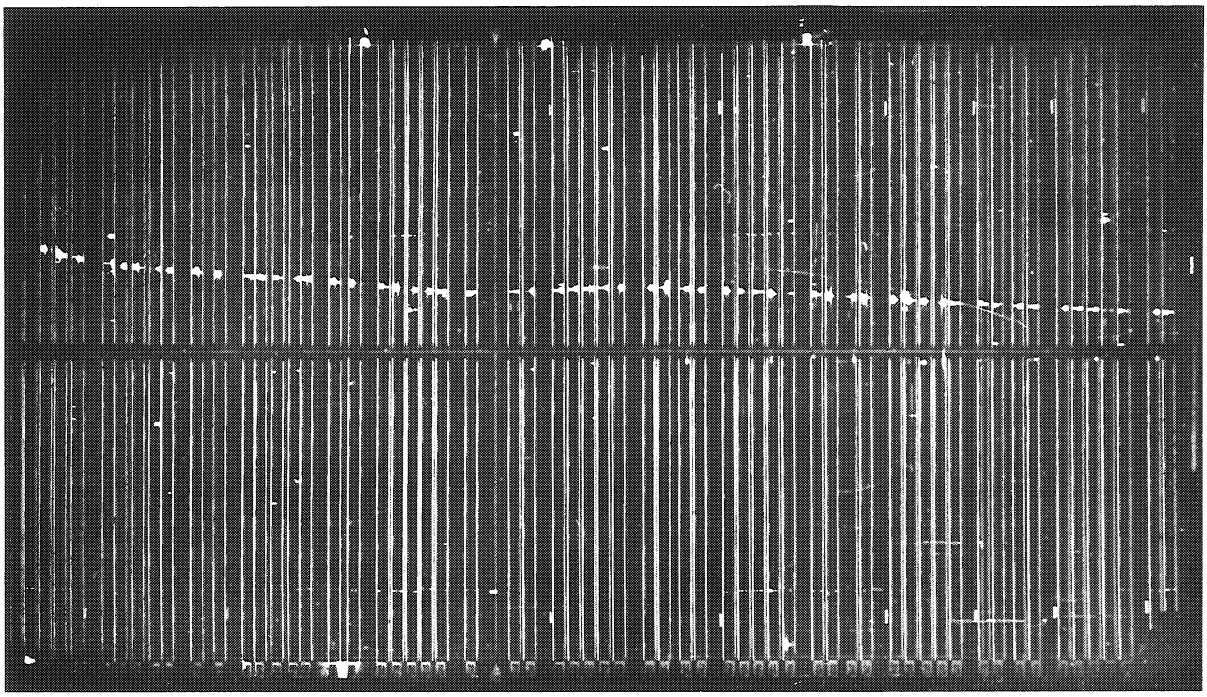

Fig. 2

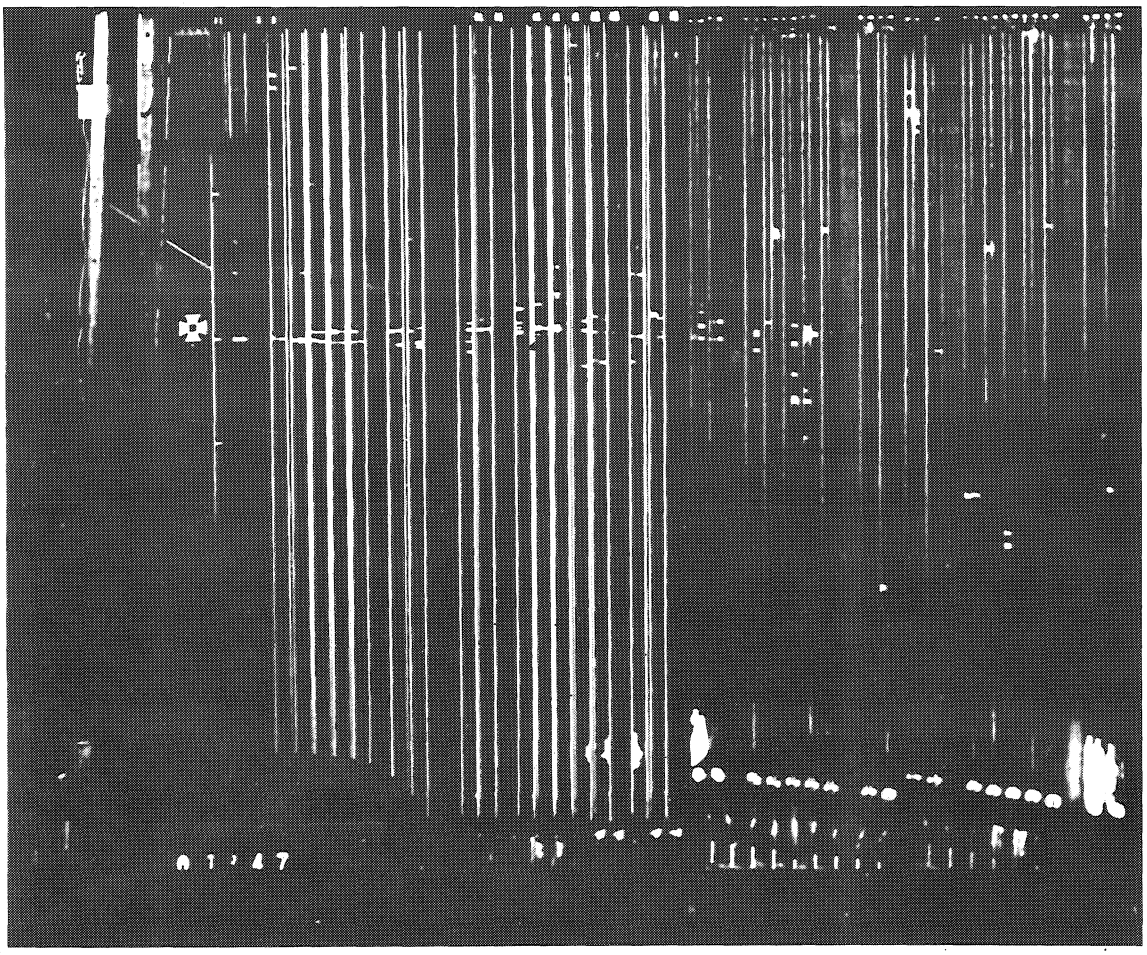

Fig. 3

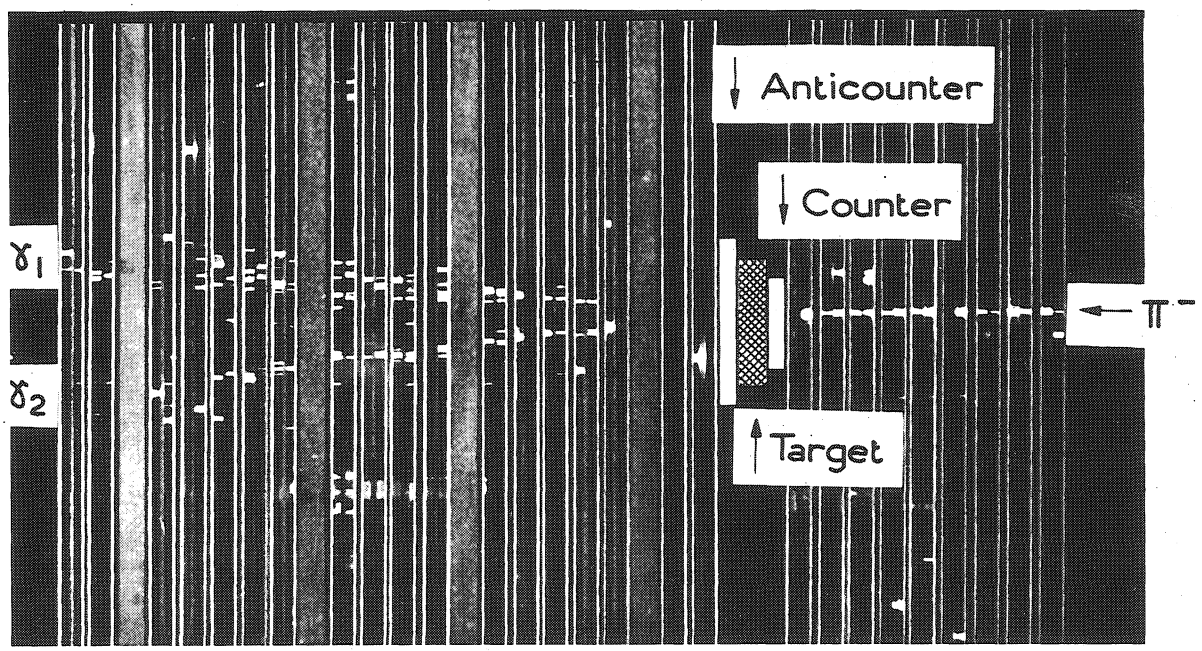

Fig. 4

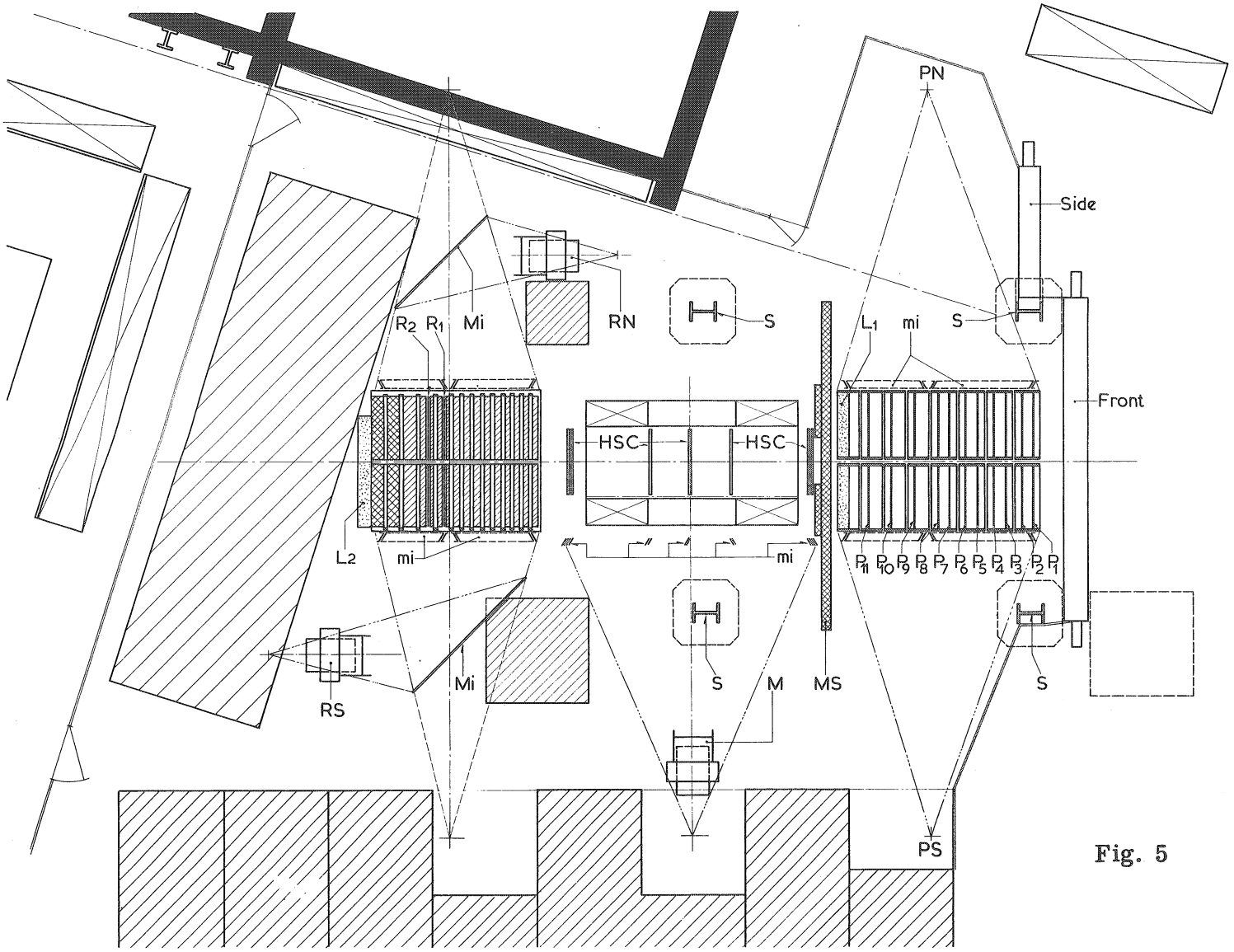

P1 – P11, R1, R2 — Plastic Counters
L1, L2 — Liquid YES Counters
Front, Side — Anti Coincidence Counters
+ — Virtual Camera Positions
PN, PS — Camera Pairs (production region north and south respectively)
RN, RS, M — Stereo Cameras (range chamber north, south and magnet)
MS — Magnetic Shielding Wall
HSC — Hodoscope Spark Chambers
mi — Small Mirror Pairs
Mi — Large Mirrors
S — Roof Support
Pb Walls
Fe Walls

Fig. 5

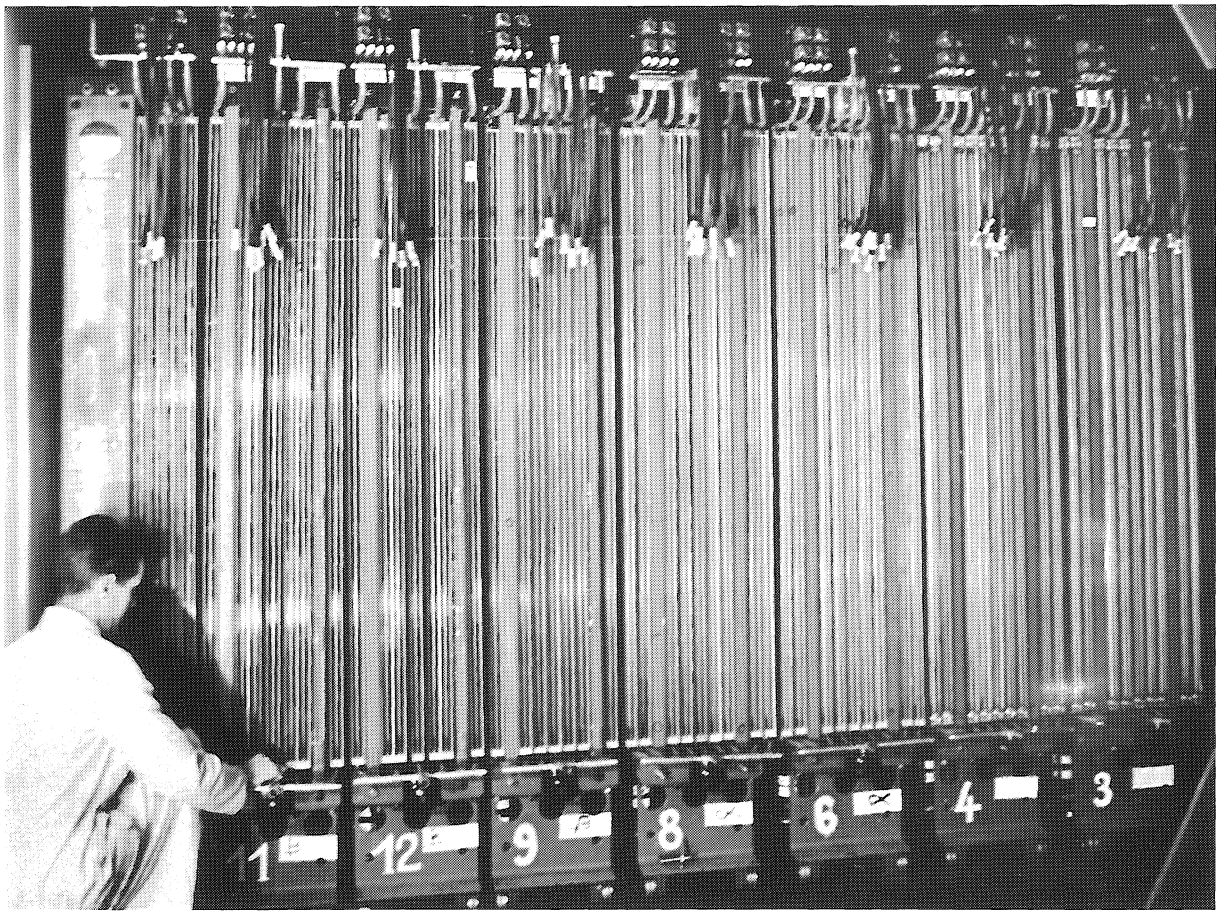

Fig. 6

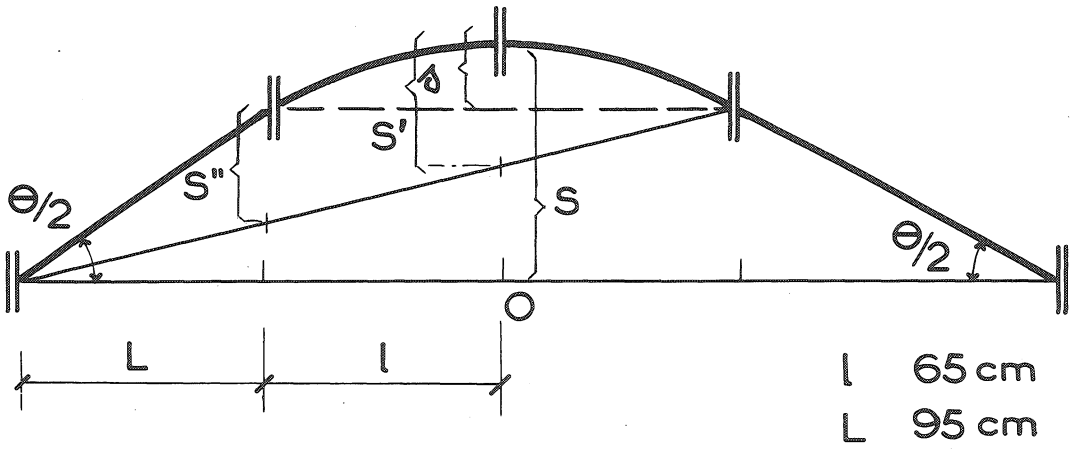

Fig. 7

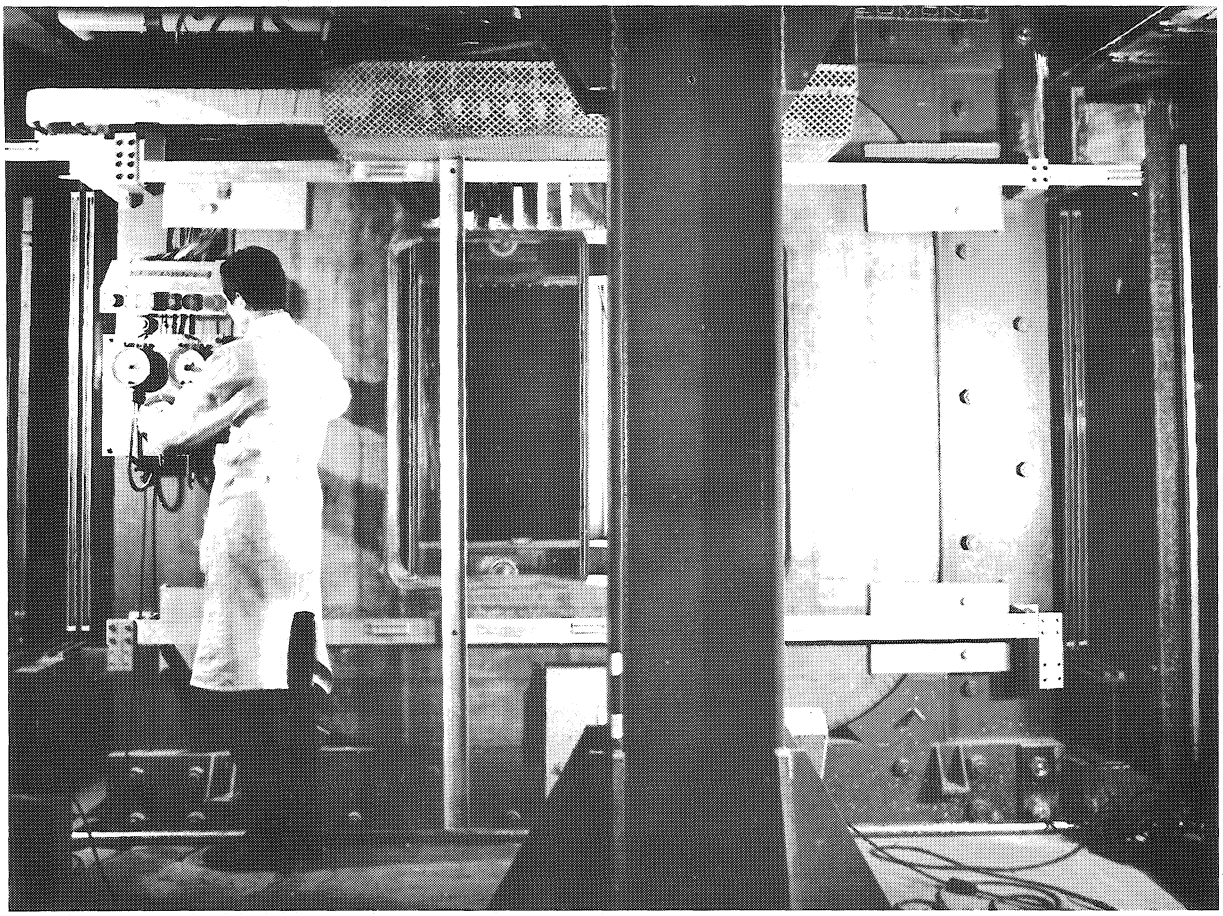

Fig. 8

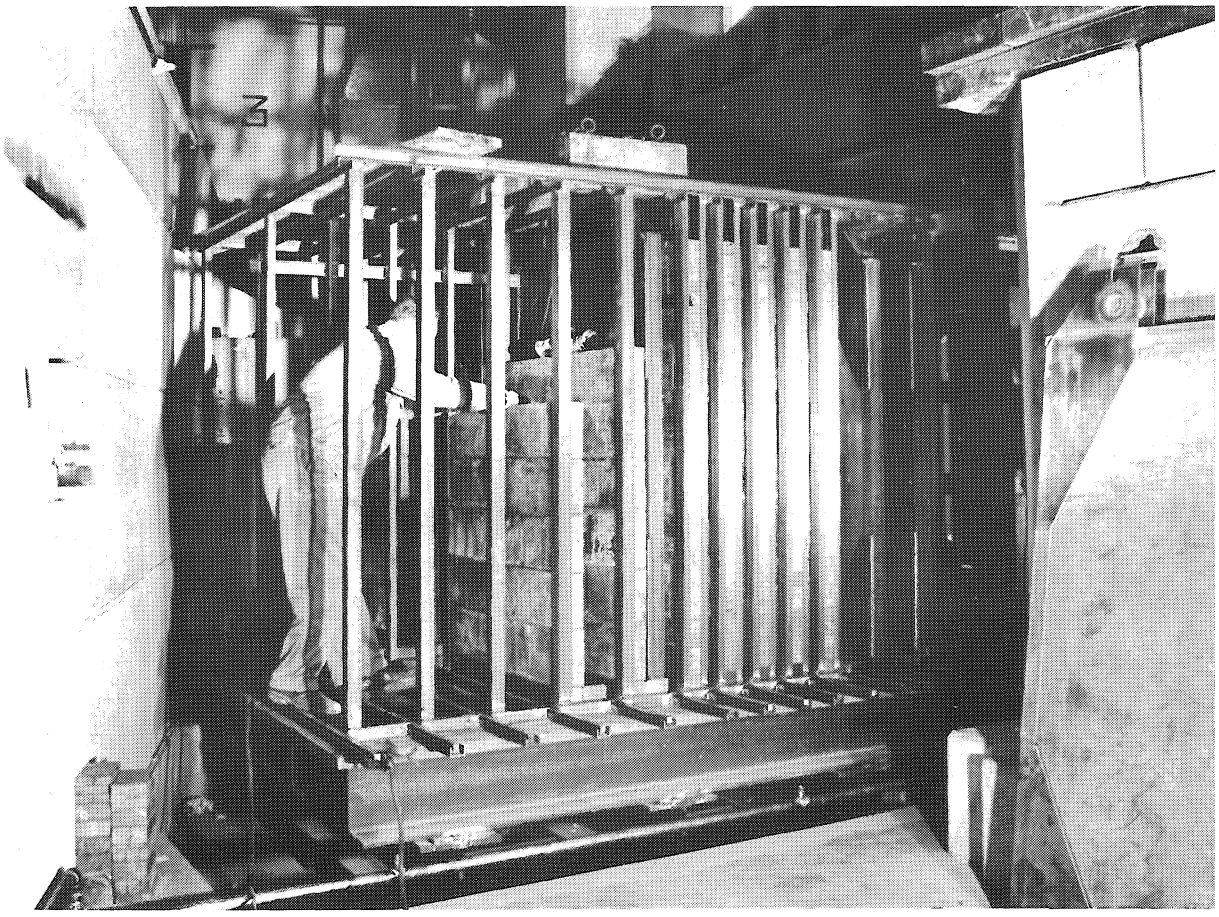

Fig. 9

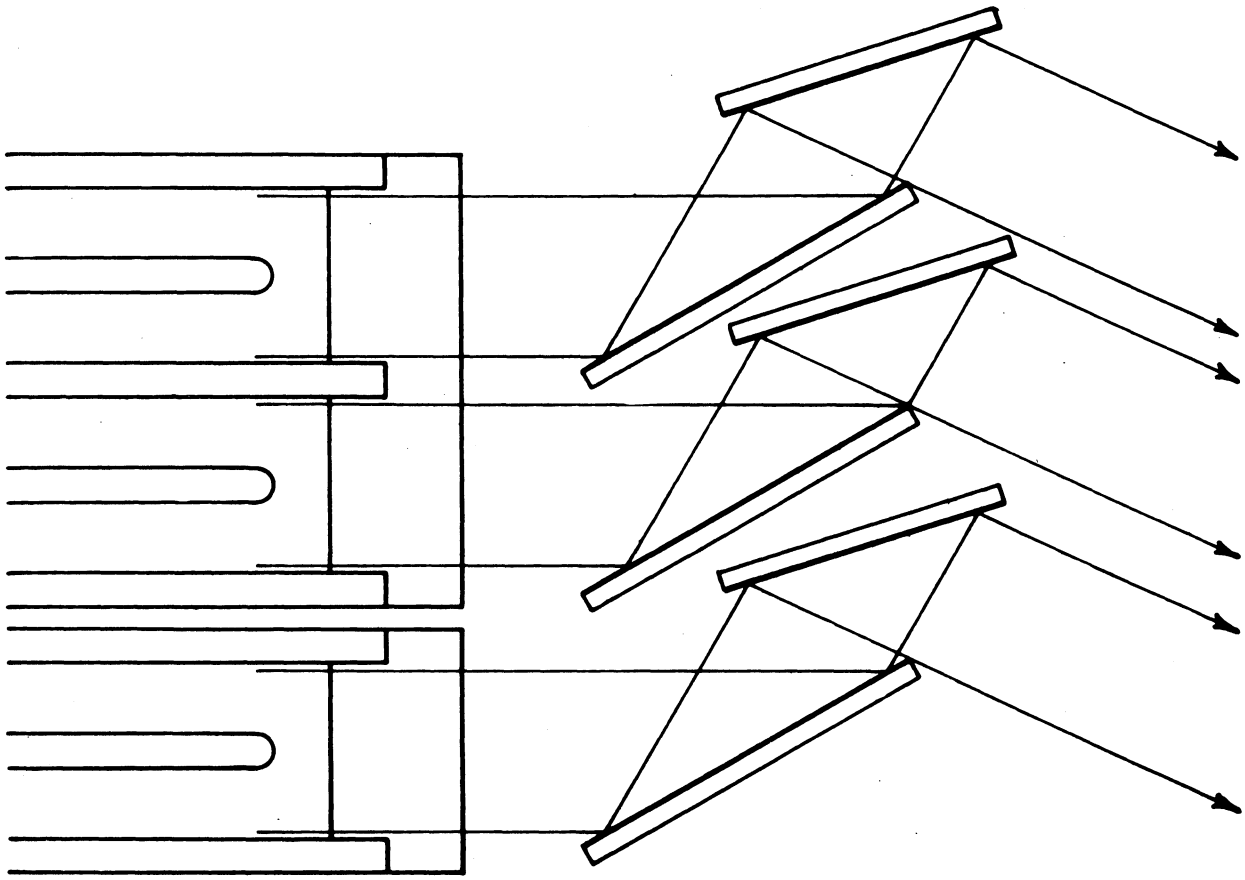

Fig. 10

FIG. 11 SCHEMATIC OF LOGICAL ELECTRICAL

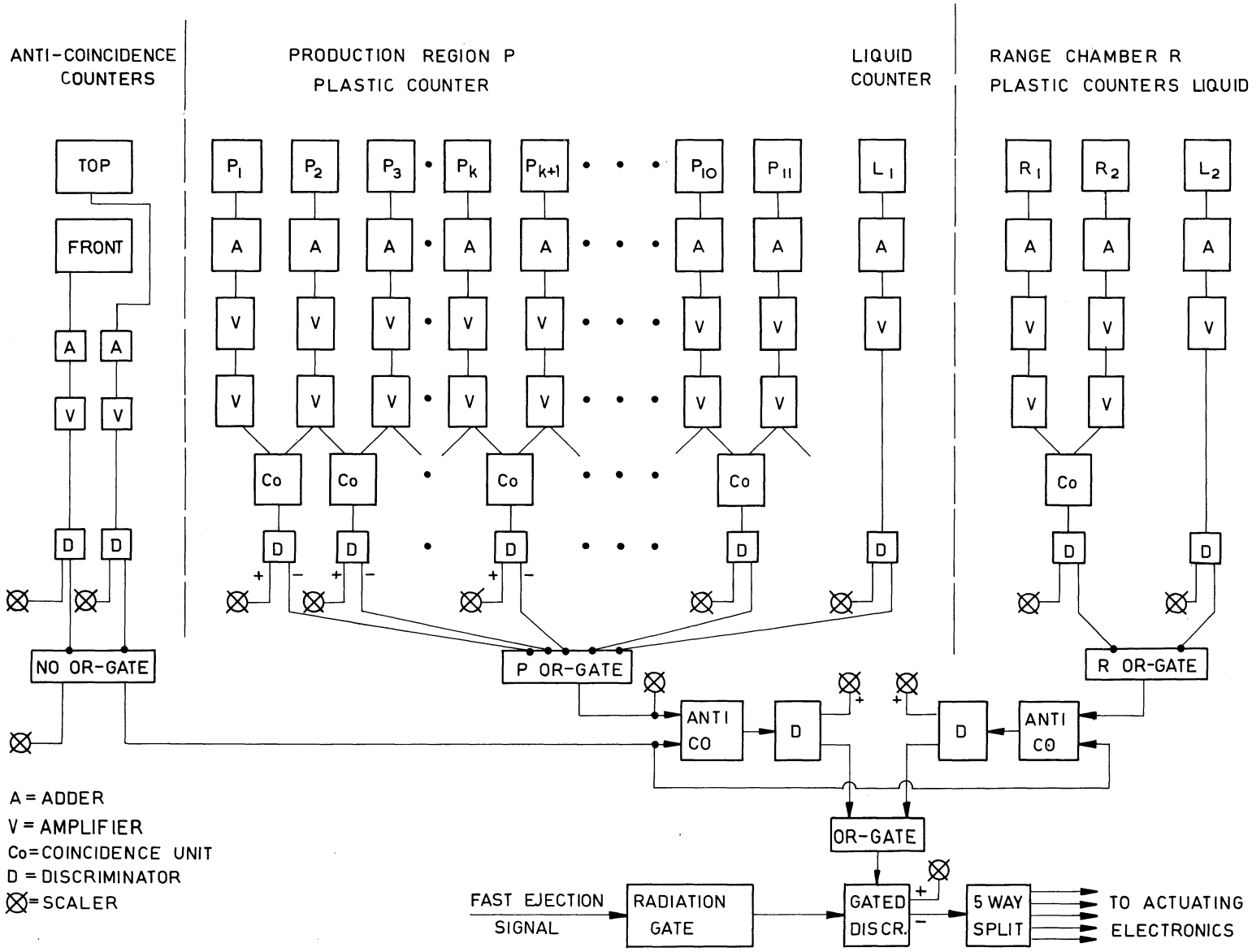

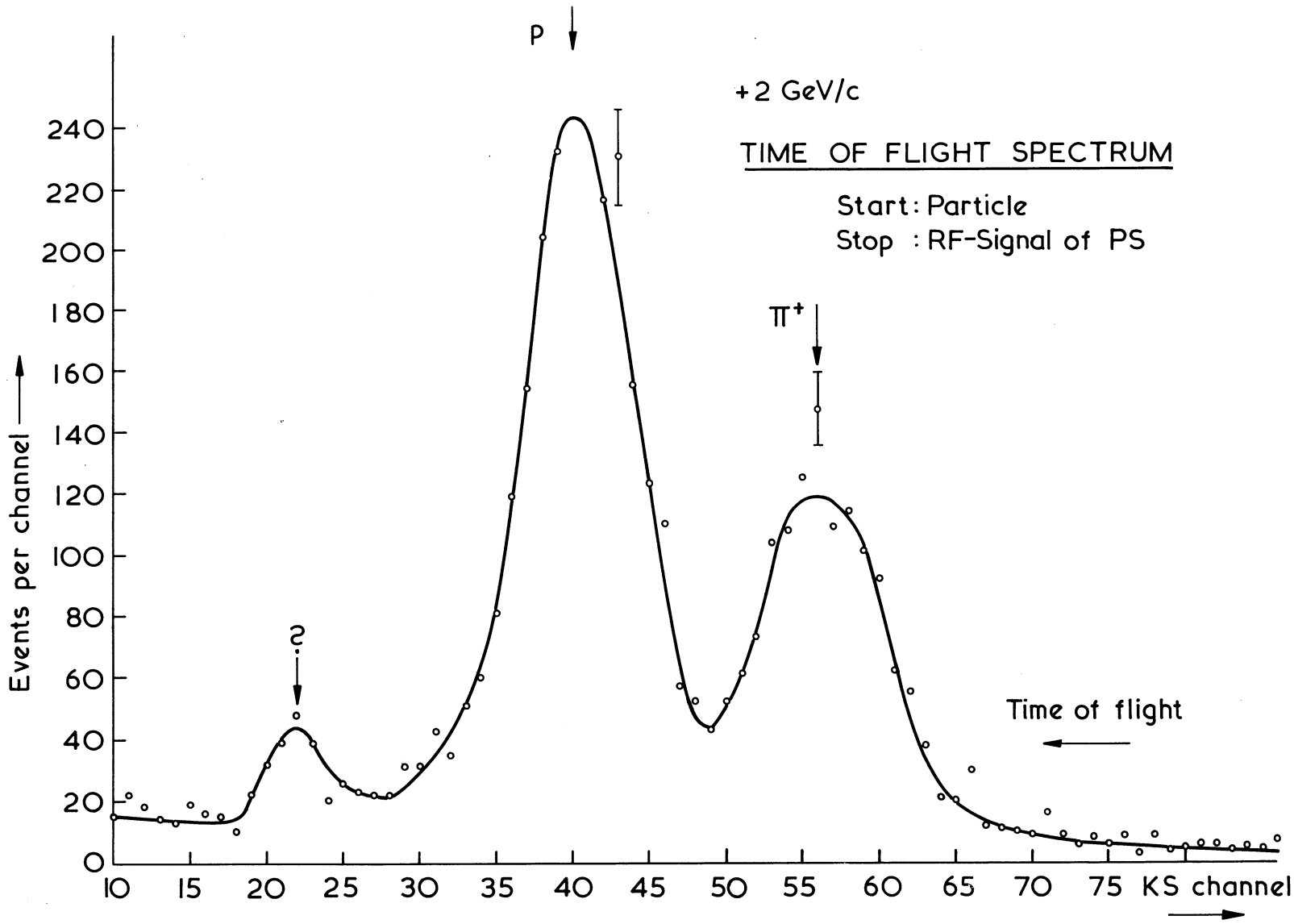

FIG. 12